agronomy

MDPI

Article

Variation in Soil Hydrothermal after 29-Year Straw Return in Northeast China during the Freeze–Thaw Process

Haiyu Li [1], Meng Li [2,*], Shuli Wang [1,*] and Ming Gao [1]

[1] School of Forestry, Northeast Forestry University, Harbin 150040, China; lihaiyu@nefu.edu.cn (H.L.); 2019023107@nefu.edu.cn (M.G.)
[2] Northeast Institute of Geography and Agroecology, Chinese Academy of Sciences, Harbin 150081, China
* Correspondence: limeng@iga.ac.cn (M.L.); shuliwang@nefu.edu.cn (S.W.)

Abstract: In seasonal agricultural frozen soil areas, the straw return may influence the freeze–thaw characteristics by changing the soil organic matter and porosity. Monitoring moisture and heat in the freeze–thaw period is significant for preventing spring waterlogging and reasonable planting arrangements. However, the effect of long-term straw return on the soil freeze–thaw process is still unclear. In this study, we investigated the dynamics of soil temperature (ST) and soil moisture (SM) between straw-return cropland (SF) for 29 consecutive years and no-fertilization cropland (NF) during freeze–thaw progress in northeast China. The soil in both sites underwent unidirectional freezing and bidirectional thawing processes. The soil freezing and thawing dates in the NF of the profile occurred earlier than that in the SF. The NF had higher frozen depth and freezing rate than the SF and exhibited a larger range of ST variation and higher heat transmission efficiency. The SM showed a declining trend before the ST started to decrease to a freezing point at different depths in both sites. The migrated SM in most soil layers decreased during monitoring. The relationship between SM and negative ST was a power function at different frozen depths. The SM decreased rapidly in the range of −2–0 °C in both sites. During phase changes, the SF and NF consumed 33.0 and 43.6 MJ m^{-2}, respectively. The results can partially explain the response of straw return to soil hydrothermal variation during the freeze-thaw process. This study may provide an integral theory for effectively utilizing agricultural soil hydrothermal resource in northeast China.

Keywords: soil moisture; soil temperature; freeze–thaw process; hydrothermal coupling; phase change

Citation: Li, H.; Li, M.; Wang, S.; Gao, M. Variation in Soil Hydrothermal after 29-Year Straw Return in Northeast China during the Freeze–Thaw Process. *Agronomy* **2024**, *14*, 1525. https://doi.org/10.3390/agronomy14071525

Academic Editor: Nicolas N. Baghdadi

Received: 13 May 2024
Revised: 5 July 2024
Accepted: 9 July 2024
Published: 13 July 2024

1. Introduction

In seasonal frozen regions, frequent freeze–thaw processes occur during the seasonal transitional period because of periodic variations in meteorological factors [1]. The freeze–thaw process is crucial for agriculture and the ecological environment as it profoundly affects soil moisture (SM) redistribution, thermal equilibrium, spring plowing, and plant germination [2]. Soil structure and moisture movement can be significantly altered by freeze–thaw cycles [3]. As soil water moves and heat transfers, the freeze–thaw process becomes more complicated than soil water transfer without freezing [4]. In general, soil temperature (ST) affects soil water characteristics [2]. Freezing forces alter the SM phase and prompt the migration of unfrozen water content to frozen soil, thus redistributing SM throughout the soil layers [5,6]. Previous studies have focused on SM characteristics and movement mechanisms during freeze–thaw progress [7,8]. The initial SM is a significant factor affecting the freeze–thaw process [2]. Chen et al. [9] investigated two types of croplands and found that the tendency of soil to freeze increases with decreasing initial SM. Meanwhile, soil texture can influence the amount of moisture transported during the freeze–thaw progress. Chen et al. [10] indicated that small soil particle size promotes phreatic moisture migration to soil water under laboratory conditions. Ala et al. [8] studied SM transport in dunes and interdune regions during freeze–thaw progress, and found that heavy clay soils migrate more moisture than sandy soils.

In agricultural freeze regions, straw management is critical to regulating ST and SM distribution in different soil layers [11]. In the freezing process, straw mulching increases upper moisture, lowers soil energy budget fluctuations, and reduces ST and SM amplitudes [12]. Moreover, straw mulching reduces frozen soil depth and delays initial freezing and melting, inhibiting soil surface evaporation [11]. Compared with uncovered soil, straw returns can reduce soil evaporation by over 49% in a completely frozen period [13]. Moreover, the length of straw returning time also affects the soil water and heat conditions. Long-term straw burial mulching increased the soil water by 0.9% and 4.4%, respectively [14]. Compared with the no-straw return treatment, 1 year, 3 years, 5 years, or 7 years of straw returning altered water conservation by 2.60–13.26% [15]. The long-term straw returning experiment changed the soil moisture content, and increased temperature and hydraulic conductivity [16]. Overall, ST and SM are complexly affected by straw mulching or straw return during the freeze–thaw progress, particularly by soil properties, local microclimates, and regional climatic conditions [17]. Consequently, specific regional studies about the soil freeze–thaw process cannot be ignored.

Regions of Phaeozems in the soil taxonomy of the World Reference Base for Soil Resources 2022 are a vital commodity grain base that maintain national food security in northeast China [18]. This area is affected by climate, and the soil freezes seasonally [19]. Influenced by natural and human factors, increased soil degradation threatens agricultural production and food availability in northeast China [20]. Straw return is an appropriate approach to improve soil quality in cropland and promote sustainable agricultural development [21]. However, the variations in ST and SM after long-term straw return in northeast China during the freeze–thaw period are still unclear. Thus, our objectives were as follows: (1) to evaluate the impacts of straw return on soil freeze–thaw characteristics; (2) to compare straw-return cropland (SF) and no-fertilization cropland (NF) in terms of SM migration; and (3) to reveal hydrothermal coupling processes in the SF and NF during the freeze–thaw process.

2. Materials and Methods

2.1. Study Area

The experimental site was established at Hailun Agroecosystems National Field Observation and Research Station (47°26′ N, 126°38′ E), located in Hailun City in Heilongjiang Province, northeast China (Figure 1a,b). The altitude is 461 m above sea level, and the climate at the study site is a cold temperate continental monsoon. The annual average temperature is about 1.5 °C, and precipitation is 500–600 mm. The average annual solar radiation is 4600 MJ m^{-2}, and the annual average available accumulated temperature (≥10 °C) is 2450 °C. The soil type is classified as Phaeozems based on WRB 2022 soil taxonomy. At the start of the experiment, the surface soil layer properties were 31.9% clay content, 1.2 g cm^{-3} bulk density, and 29.6 g kg^{-1} SOC; the middle layer properties were 37.6% clay content, 1.3 g cm^{-3} bulk density, and 13.7 g kg^{-1} SOC; and the lower layer properties were 40.1% clay content, 1.4 g cm^{-3} bulk density, and 5.0 g kg^{-1} SOC.

2.2. Methods

A positioning experiment of soybean and maize rotation was conducted in 1990. Two cropland sites were studied: SF (straw-return and fertilization treatment; the fertilizer returns to the plot along with the total aboveground biomass) and NF (no-fertilization treatment). The experimental plots were close to each other, and the area was 30 m × 60 m (Figure 1c). Rototillers incorporated crop straws and fertilizers into the soil after harvest in October. The fields were fertilized with NPK fertilizers in early May every year before sowing. The NPK fertilizers were urea, ammonium hydrogen phosphate, and potassium sulfate applied at 112.5, 19.7, and 49.8 kg ha^{-1} y^{-1}. In a ratio of 1:2, urea was used as a basal fertilizer and top dressing. Basal fertilizers were ammonium hydrogen phosphate and potassium sulfate.

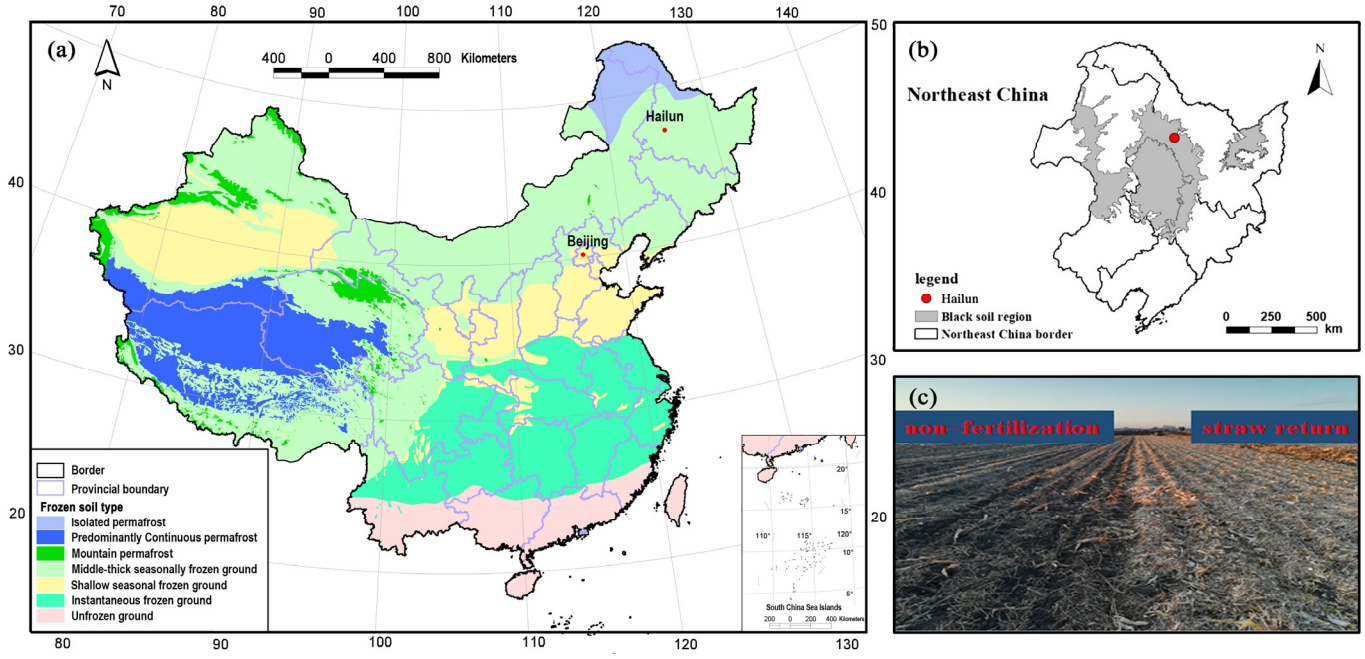

Figure 1. Permafrost types distribution map in China (**a**), location of the study area (**b**), and the monitoring schematic of straw-return cropland (SF) and no-fertilization cropland (NF) (**c**).

Daily meteorological data were collected through an automatic meteorological station near the plot. The ST and SM were monitored using the Chinese Ecosystems Research Network Automatic Soil Moisture Station (Beijing Truwel Instruments, Beijing, China) with a battery-powered data logger (A755 SDI12/ModBus GPRS Telemetry Datalogger; Adcon Telemetry Group, Vienna, Austria) and 10 probes (Hydra Probe Soil Moisture Sensors). The 10 probes were placed at each plot to measure the ST and SM at 10, 20, 30, 40, 60, 80, 100, 120, 150, and 180 cm soil depths. We recorded the ST and SM every 30 min, and the measured SM was the unfrozen water content. The freeze–thaw monitoring period was from 1 November 2019 to 31 May 2020. Figure S1 shows the variations in precipitation and air temperature from 31 May 2019 to 31 May 2020.

Using diurnal ST variations in each layer, we identified three stages of the freeze–thaw process: the initial freezing process (the diurnal minimum ST lower than 0 °C), completely frozen process (the diurnal maximum ST lower than 0 °C), and the thawing process (the diurnal minimum ST lower than 0 °C and the maximum ST higher than 0 °C).

2.3. Data Analysis

All ST, SM, and air temperature data were analyzed using 24 h averages. The normality and homogeneity of variance, the Kolmogorov–Smirnov (K-S) test, and Levene tests were performed on all variables, and data were log-transformed as necessary to meet the assumption of statistical analysis. Subsequently, we used independent samples *t*-tests to analyze the significantly differences in SM variations and mean ST between SF and NF at each soil layer, and Duncan's test to perform significance tests on the mean ST across different soil layers at the same site. Regression analysis was used to compare the effects of air temperature on NF and SF temperatures during the monitoring period. All data analyses were performed using SPSS 22.0, and all the figures were plotted with Origin 8.1 software.

The freezing or thawing rate was calculated as follows:

$$R_i = \frac{H_{i+1} - H_i}{D_{i+1} - D_i} \quad (1)$$

where i is the ith soil depth, R_i is the freezing or thawing rate at the ith soil depth (cm d^{-1}), H is the soil thickness (cm), and D is the freezing or thawing date.

For ST and SM, the following formula was used [22]:

$$\Theta = a(-T)^b, \quad (2)$$

where θ is the unfrozen water content (cm^3 cm^{-3}), T is the negative temperature during the soil-freezing processes (°C), and a and b are empirical coefficients. SM variation was analyzed using Equation (2) with decreased ST during the freezing periods.

Heat consumption during moisture–ice phase transition was estimated using ST and SM with the following assumptions [23]:

(1) The water freezes at 0 °C, and the latent heat is 333.6 kJ kg^{-1}.
(2) Neither surface water infiltration nor transport between soil layers is considered after soil freezing. The unfrozen water content and vertical migration rates are extremely low [24].
(3) The heat of the freezing phase transition is equal to the heat of the thawing phase transition (i.e., the freezing moisture melts completely into liquid moisture during the thawing period).

$$L = \frac{1}{2} Q \rho_w \sum_i^n (\theta_i + \theta_{i+1})(z_{i+1} - z_i), \quad (3)$$

where L represents the latent heat consumed during the phase transition from water to ice (J m^{-2}), Q is the latent heat of the freezing (333.6 kJ kg^{-1}), ρ_w is the density of moisture (1000 kg m^{-3}), n represents the number of soil layers, i is the ith soil depth, θ is unfrozen water content (cm^3 cm^{-3}), and z is the soil layer thickness (m).

3. Results

3.1. Variation Characteristics of the ST during the Freeze–Thaw Period

3.1.1. Characteristics of the Freeze–Thaw Processes

Figure 2 shows the variations in frozen depths and isotherms at each soil layer during the monitoring process. The soil freezing–thawing processes followed similar trends in both sites. In addition, the freezing depths of the SF and NF reached over 120 and 150 cm, respectively (Figure 2). The soil freezing date was delayed by increasing the soil layer in both sites. The 10 cm soil depth in the SF and NF started to freeze on November 3 and 4, 2019, respectively (Figure 3). At soil depths of 0–120 cm, the freezing in the SF occurred 25 days later than that in the NF.

The soil thawing processes were bidirectional in the two sites. Soil thawing in the NF and SF occurred on 19 and 20 March 2020, respectively, at the upper soil depth (Figure 3). The soil began to thaw at 120 cm after the melting soil depth reached 40 cm in the SF, whereas the soil started to melt at 150 cm at a melting soil depth of 20 cm in the NF. In both the SF and NF, the soil depth at 100 cm exhibited the latest thawing. The thaw start date in the SF was 20 March 2020, 1 day later than that in the NF. The full thawing date in the SF was 6 days later than that in the NF.

The soil layers in both sites had different freezing and thawing rates during freezing and thawing progress (Table 1). The maximum freezing rate was 2.5 and 3.33 cm d^{-1} at 10–20 cm depth in the SF and NF, respectively. However, the maximum thawing rate was 5 cm d^{-1} at 80–100 depth in the SF and 20 cm d^{-1} at 100–120 depth in the NF. Furthermore, the average freezing and thawing rates in the 120 cm soil profile in the SF were 1.42 and 1.58 cm d^{-1}, whereas those in the NF in the 150 cm soil profile were 1.53 and 1.59 cm d^{-1}, respectively.

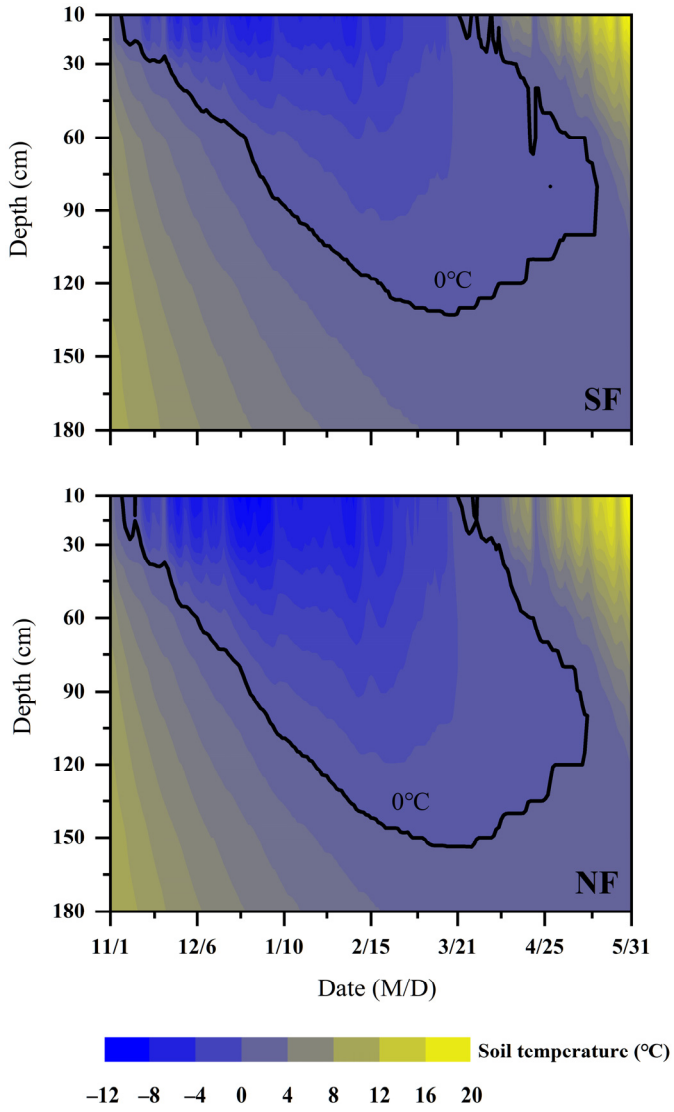

Figure 2. Isothermals of soil profile in the SF and NF during the monitoring process.

Table 1. Freezing and thawing rates at each depth in the NF and SF.

Depth (cm)	SF		NF	
	Freezing Rate (cm d^{-1})	Thawing Rate (cm d^{-1})	Freezing Rate (cm d^{-1})	Thawing Rate (cm d^{-1})
10–20	2.5	0.83	3.33	1.67
20–30	0.56	2.5	1.43	1
30–40	2	1	0.91	3.33
40–60	0.77	1.11	1.82	2
60–80	2.22	2.86	1.11	1.18
80–100	1.11	5	1.82	2.22
100–120	0.77	0.57	1.05	20
120–150			0.77	0.81

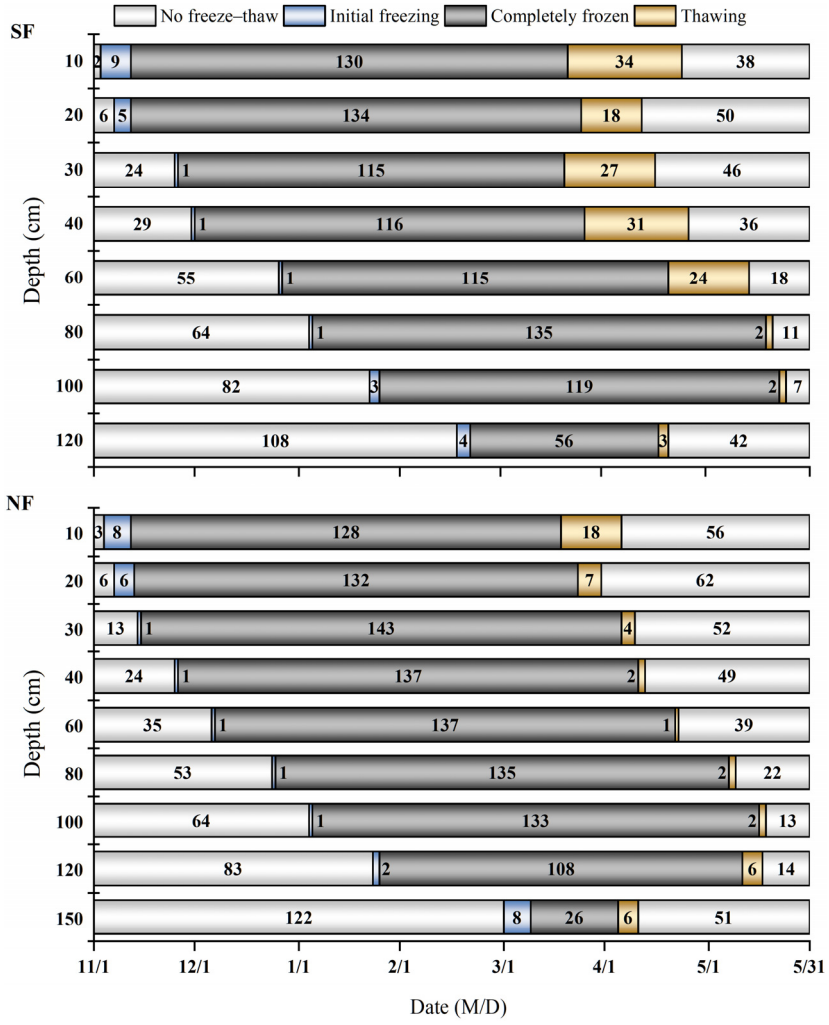

Figure 3. The temporal distribution of the various freeze–thaw stages at each soil depth in the SF and NF.

3.1.2. Variation Process of the ST

Table 2 shows the average temperatures during the three stages of the freeze–thaw process and the minimum temperatures during the entire freeze–thaw period. The minimum ST during the freeze–thaw progress represents the soil freezing intensity [25]. An increased minimum freezing ST was observed with increasing soil depth, and was investigated in the completely frozen period in both sites (Table 2). Additionally, the SF exhibited a higher minimum ST than the NF across all soil layers (Table 2). Figure 4 shows that the mean ST increased with soil depth during the monitoring period. The mean ST in the SF and NF ranged from −1.2 °C to 2.9 °C and −1.7 °C to 2.7 °C, respectively. At depths of 80–120 cm, the mean ST in the SF was significantly higher than that in the NF.

Figure 5 describes the amplitude of soil temperature variations at various depths in the SF and NF during the entire freeze–thaw period. The ST varied with depth in a logarithmic manner in both sites. A decrease in the ST was observed with increasing soil depth in the SF and NF. The range of variation in ST in the SF and NF was 7.7 °C to 27.6 °C and 8.8 °C to 30.4 °C, respectively. Overall, the range of ST variations in the NF was larger than in the SF at each soil layer.

Table 2. Average and minimum temperatures at different soil freeze–thaw stages.

Site	Soil Depth (cm)	Average Freezing Temperature (°C)	Average Frozen Temperature (°C)	Average Thawing Temperature (°C)	Minimum Temperature (°C)	Date of Minimum Temperature
SF	10	−0.46	−5.49	2.02	−8.96	12/27
	20	−0.22	−4.61	0.22	−7.43	12/27
	30	−0.17	−3.43	−0.27	−5.48	2/8
	40	−0.05	−2.70	−0.16	−4.67	2/8
	60	−0.02	−1.38	−0.04	−2.70	2/9
	80	0.01	−0.82	0.04	−1.90	2/10
	100	−0.01	−0.47	0.07	−1.10	2/19
	120	−0.01	−0.18	0.04	−0.30	3/15
NF	10	−0.51	−6.81	0.35	−11.55	12/27
	20	−0.34	−6.08	0.11	−10.39	12/27
	30	−0.27	−4.93	0.10	−8.89	1/1
	40	−0.21	−3.81	0.01	−6.67	2/8
	60	0.06	−2.41	0.04	−4.80	2/9
	80	−0.06	−1.58	0.05	−3.40	2/10
	100	−0.04	−0.99	0.04	−2.20	2/10
	120	0.05	−0.60	0.04	−1.31	2/23
	150	−0.01	−0.07	0.05	−0.10	3/11

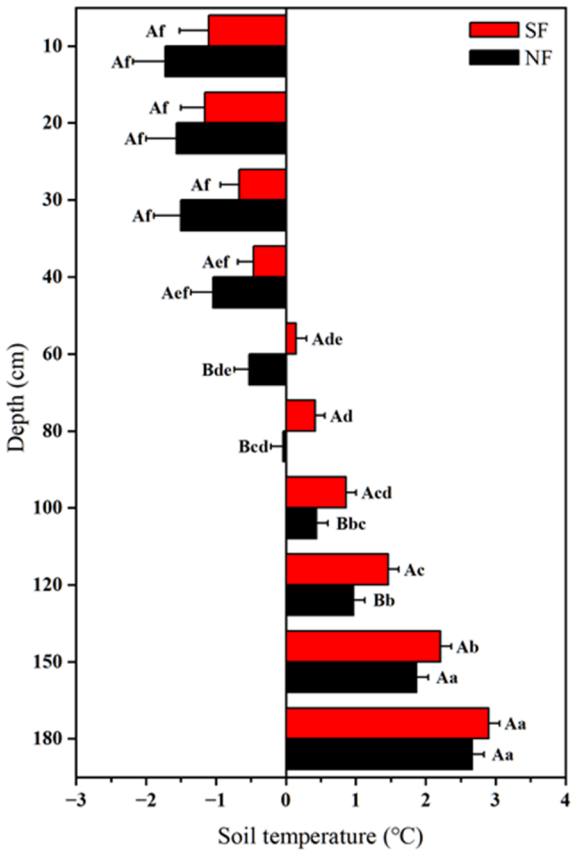

Figure 4. Vertical distribution of mean soil temperature in the SF and NF. Different capital letters are significant at the same layer ($p < 0.05$); different lowercase letters in one profile indicate a significant difference ($p < 0.05$).

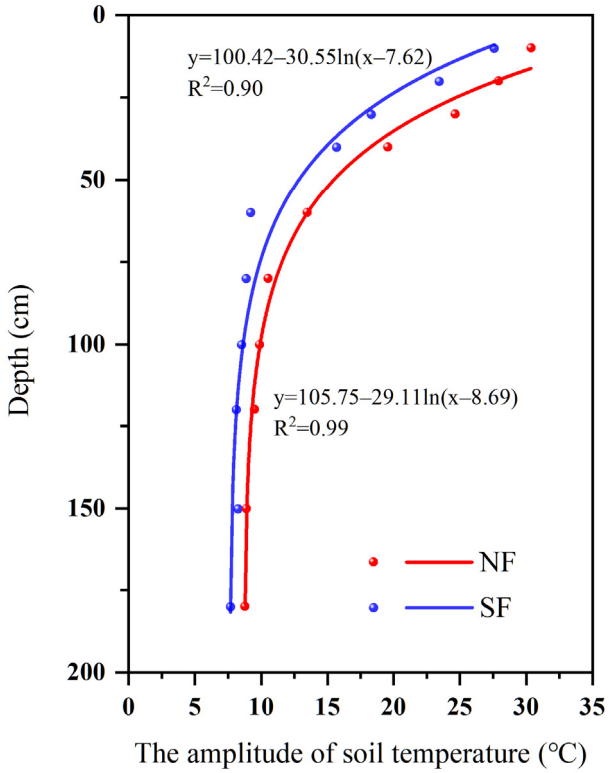

Figure 5. Variations in the soil temperature range at various depths and fit curves in the SF and NF during the monitoring period.

3.1.3. Relationship between ST and Air Temperature

The variation tendency of ST was identical to air temperature, showing a trend downward initially and then rising at 0–100 cm soil depth in both sites during the monitoring process (Figure 6). The ST and air temperature were significantly correlated, except at 80 cm depth in the SF and the 100 cm layer in the NF, respectively ($p < 0.01$; Table S1). The ST was significantly linearly related to air temperature in the surface 40 cm soil depth, and correlation coefficients decreased with increasing soil depth ($p < 0.01$; Figure 7). The R^2 for the NF was higher than that for the SF at the upper 40 cm soil depth. The coefficient 'a' measures the soil and air thermal efficiency [2]. A high value of 'a' corresponds to a fast heat transfer between air temperature and ST. The parameter 'a' in the SF was smaller than that in the NF at the upper 40 cm soil depth (Table S1).

3.2. Soil Moisture Transport during the Freeze–Thaw Period

3.2.1. Variation Process of the SM

As Figure 8 shows, SM variations had similar patterns in the two study sites at different soil depths, showing a downward–stable–upward trend during the monitoring period. The SM decreased in both sites before the ST reached freezing temperatures at each soil depth. On 19 and 20 March, the SM started to fluctuate considerably at different soil layers in the NF and SF, respectively. The mean SM in the initial freezing and thawing periods in the frozen soil profiles was higher than that in the completely frozen period at 0–120 cm soil layers. From the initial freezing period to the completely frozen period, the SM in the SF and NF decreased by 15.7% to 60.6% and 15.6% to 56.8% at 0–120 cm soil depths, respectively. During the thawing stage, the SM at 0–120 cm soil depths increased by 22.7% to 139.4% and 1.31% to 81.2% in the SF and NF, respectively.

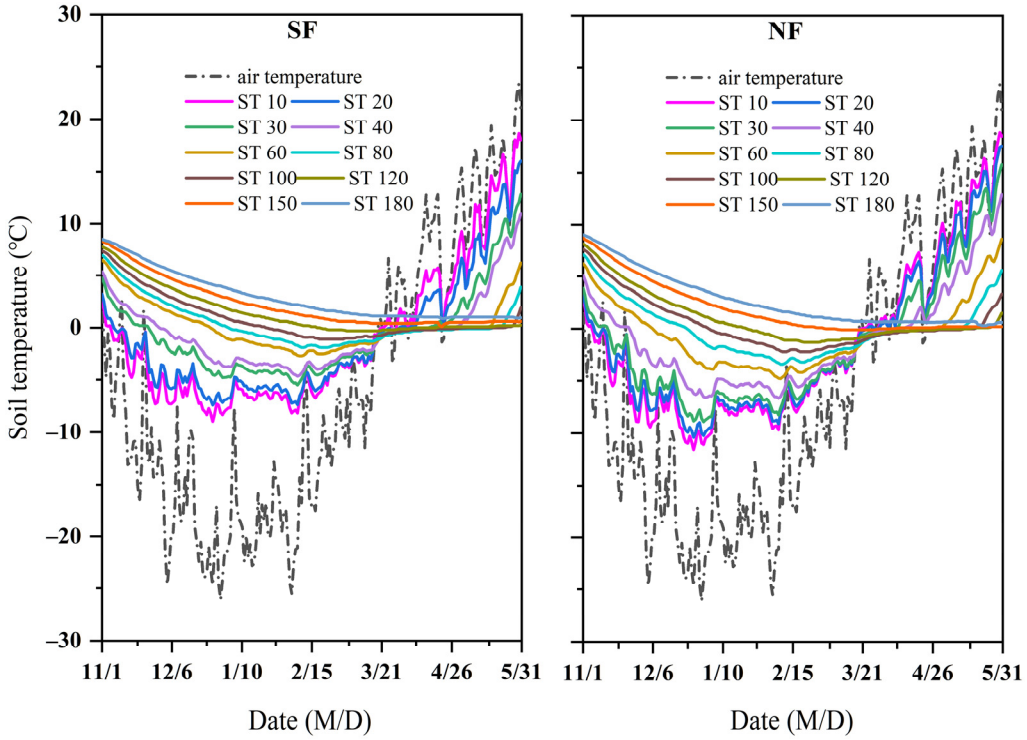

Figure 6. Dynamics of soil temperature and air temperature in the SF and NF during the monitoring period.

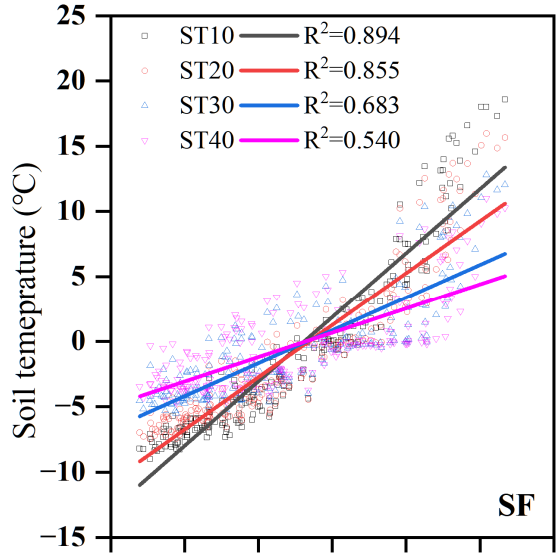

Figure 7. *Cont.*

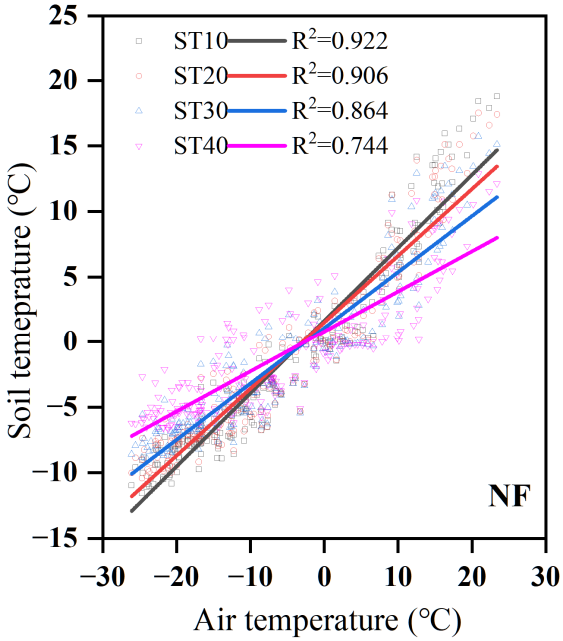

Figure 7. Correlation between air temperature and soil temperature at 0–40 cm depths in the SF and NF.

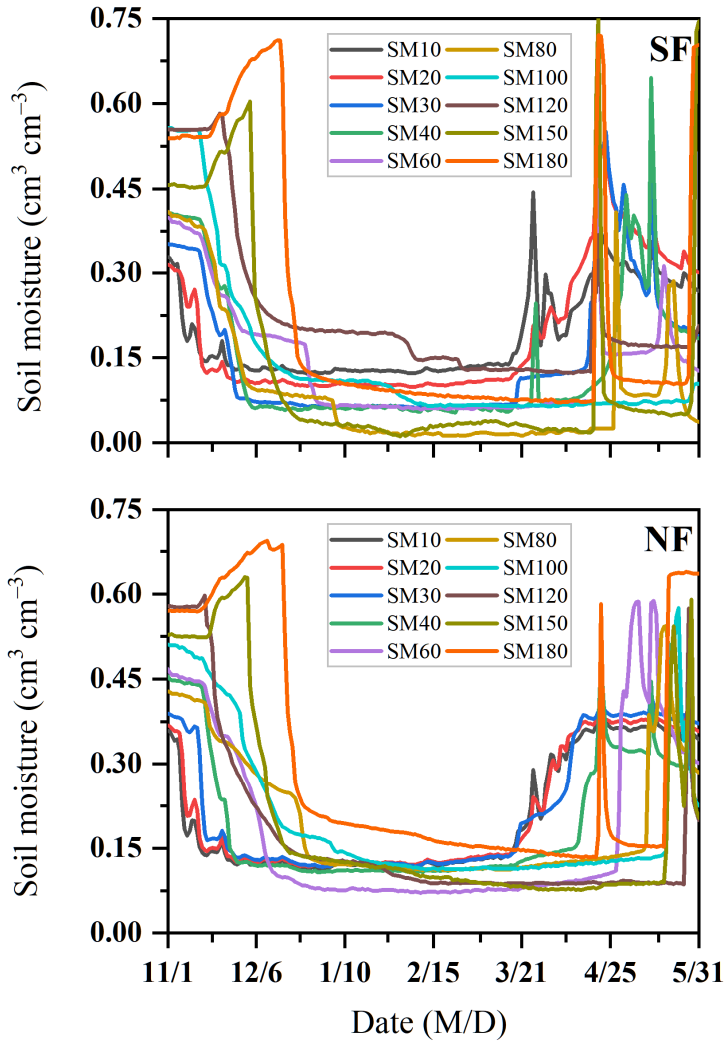

Figure 8. Dynamic variations in soil moisture at different layers in the SF and NF.

3.2.2. Movement of SM

The SM in the initial time indicates the SM on the day before the initial freezing period, and the SM in the final time represents the SM on the day after the thawing period. Our results showed that SM migration resulted in variations in SM between the initial and final times (Figure 9). The amounts of migrated moisture in the SF and NF were 0.027–0.485 and 0.003–0.490 cm^3 cm^{-3}, respectively. The SM in the final time was lower than the SM in the initial time, except at 20 cm depth in the SF, and the SM at 100 cm depth showed the highest decrease (9.7 mm in the SM storage). By contrast, the SM in the NF decreased at 30–180 cm, except at 80 and 180 cm depths, and the reduction at 120 cm depth was the highest (9.8 mm in the storage).

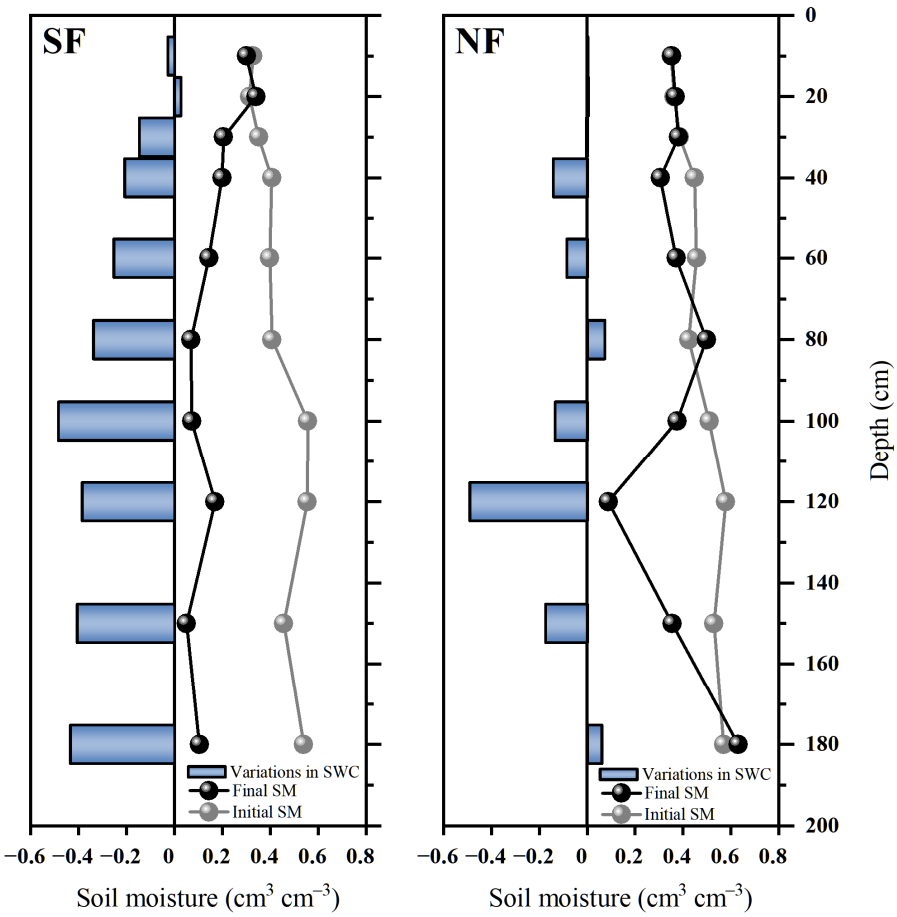

Figure 9. Movement of soil moisture at each soil depth in the SF and NF.

3.3. Soil Water–Heat Coupling Process Characteristics during the Freeze–Thaw Period

3.3.1. SM and ST during the Freezing Period

Based on Equation (2), the relationship between SM and negative ST during the freezing period is established in Figure 10. SM showed power function relationships with ST at different depths, with coefficients of −0.021–0.841 in the SF and −0.032–0.842 in the NF (Figure 10 and Table S2). The SM decreased rapidly in the range of −2–0 °C in the two sites. At the 10–30 cm soil depth, the slope of the declining trend was steeper than that in the lower soil layers in the SF and NF.

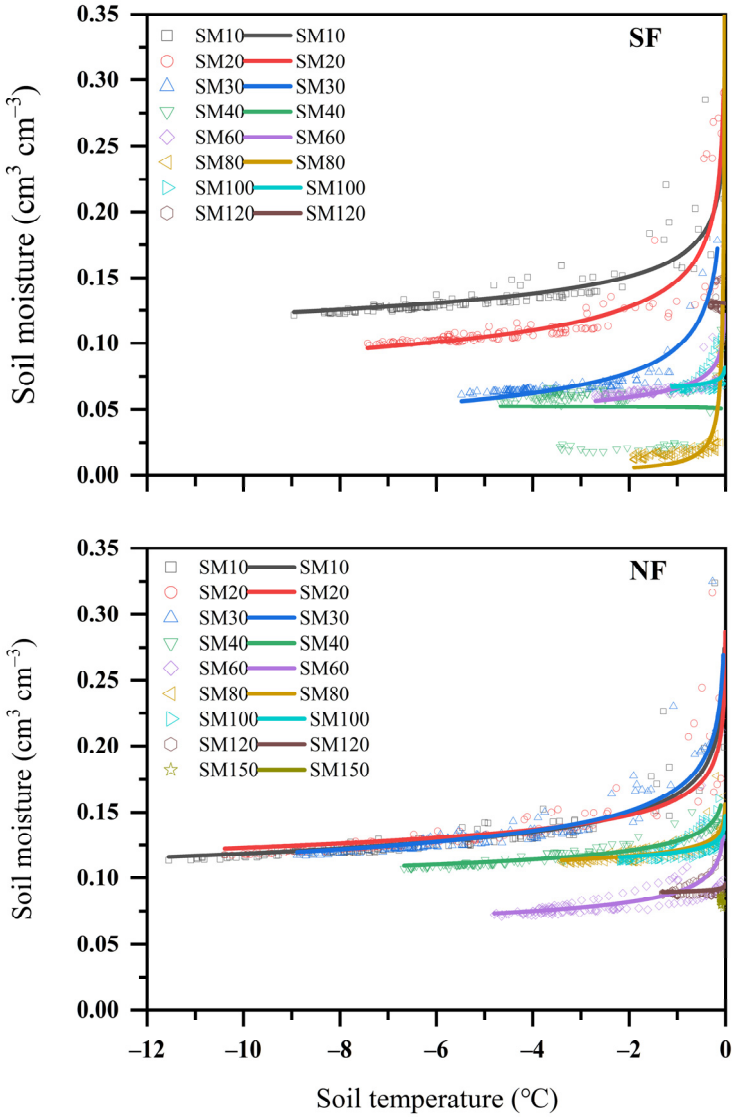

Figure 10. Fitting curves of soil moisture vary with soil temperature.

3.3.2. Energy from Phase Transitions during the Freezing Stages

We calculated the amount of energy required to change the water phase from unfrozen to ice by using SM and ST [23]. Based on the assumptions mentioned in Equation (3), the initial unfrozen soil moisture (ISM) is the SM corresponding to the soil-freezing temperature at each soil depth, and the termination unfrozen soil moisture (TSM) refers to SM that kept steady at various depths when the ST reached the minimum value (Figure 11a). Figure 11b shows the difference between the ISM and TSM at each soil depth in both sites. This difference represented the moisture of the liquid–solid phase change in the SF and NF, and was calculated by the phase of moisture-to-ice integral curves [26]. The liquid–solid phase changes were 0.185 (SF) and 0.261 m^3 m^{-2} (NF), and the heat was 33.0 and 43.6 MJ m^{-2}, respectively (Table 3).

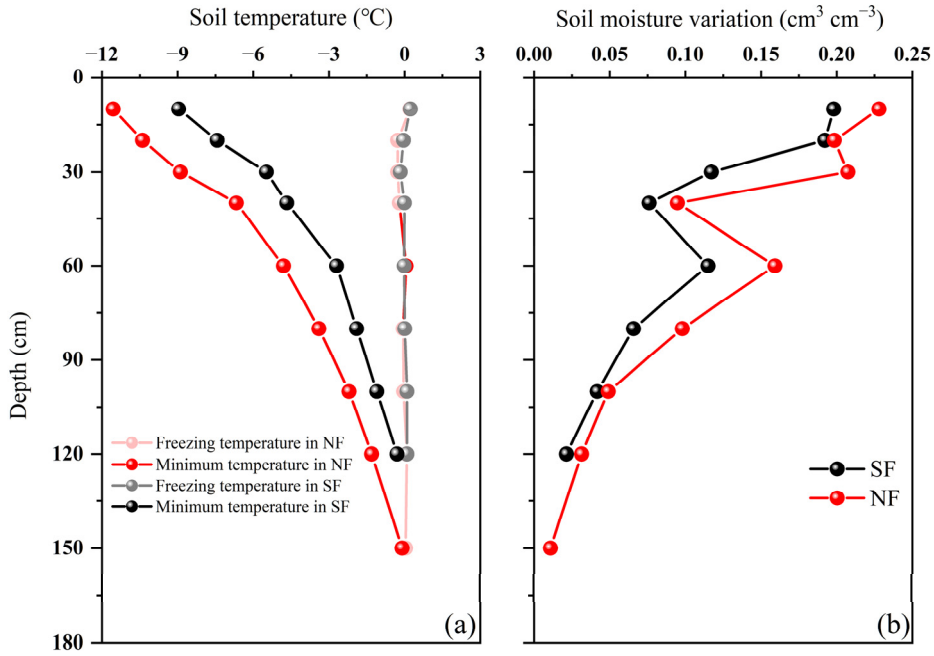

Figure 11. Soil minimum and freezing temperatures in the SF and NF (**a**), and variations in soil moisture at each soil layer of the SF and NF during the freezing stages (**b**).

Table 3. Phase changes consumed during the freeze–thaw period.

Site	Soil Depth (cm)	Moisture to Ice Phase Variable (m^3 m^{-2})	Moisture to Ice Phase Change Heat (m^3 m^{-2})
SF	120	0.185	33.0
NF	150	0.261	43.6

4. Discussion

4.1. Soil Temperature Characteristics Response to Long-Term Straw Return during the Freeze–Thaw Process

After long-term straw return, soil freezing–thawing processes differed in terms of initial freezing and thawing time, frozen depth, freeze–thaw rate, and heat transfer efficiency. Freezing and thawing in the SF from topsoil to the 120 cm depth occurred later than those in the NF (Figure 3). The reason was that, after long-term straw return treatment, the straw covering the soil surface served as insulation, preventing soil freeze–thaw cycles and slowing down soil heat loss [7]. Wang et al. [11] proposed a similar finding: straw return delayed thawing and decreased the freezing rate. Our results showed that long-term straw return reduced the freezing depth, also demonstrating straw's positive role in enhancing soil freezing resistance (Figure 2). Moreover, during the observation period, the soil temperature variations in both SF and NF exhibited a consistent pattern. Owing to the soil's large heat capacity and resistance to conduction, the surface temperature decreased slowly [27]. Consequently, the occurrence time of the minimum ST lagged as the soil depth increased (Table 2). SF and NF exhibited bidirectional melting processes (Figure 2), consistent with previous studies [2,9]. This is because the subsurface heat flow and surface temperature jointly influenced the thawing process [25]. As the air temperature rose rapidly, the soil temperature below the frozen layers stabilized, creating a greater temperature gradient in the topsoil and thus dominating the thawing process from topsoil to lower layers [28] (Figure 3). Long-term straw return reduced the soil-freezing rate, freezing intensity, and temperature fluctuation amplitude (Tables 1 and 2, and Figure 5). Straw return impeded energy transfer, leading to smaller soil energy fluctuations, thereby reducing heat exchange with the atmosphere [11].

4.2. Impact of Freeze–Thaw Process on the Movement of Moisture

The SM showed a decrease before the soil had freezing temperatures in both sites (Figure 8). This result was the same as previous observations [2,3,9]. The gradient in the soil substrate caused unfrozen water content to migrate toward the freezing front when the soil froze [29]. Moisture phase transition influences differences in SM in different freeze–thaw stages [3]. Soil water went from liquid to solid to liquid in the freeze–thaw period [30]. Thus, the SM in the initial freezing and thawing processes was higher than that in the completely frozen process at most depths in both sites (Figure 8). In the thawing stage, moisture is in a solid–liquid alternation owing to dramatic variations in ST. Hence, the SM fluctuated relatively in the soil profiles during the thawing process (Figure 8). The initial and final SM revealed the process of moisture redistribution at different soil layers [31]. SM in most soil layers decreased in the SF and NF (Figure 9). This finding differed from that of the study on the Loess Plateau [2]. Differences in soil texture may explain the difference [8]. The soil in northeast China had a higher clay content and poor permeability. Moreover, the clay content increases with soil depth until the waterproof layer is created. The waterproof layer impedes vertical water transfer, causing the accumulation of SM in some soil layers [3].

4.3. Hydrothermal Coupling during the Freeze–Thaw Process

The power function is one of the most common numerical algorithms for analyzing the relationship between SM and ST [26,32]. The relationship between SM and negative ST indicates that ST significantly influences SM (Figure 10). As ST declined, partial liquid moisture transformed into ice, and SM gradually decreased until it became stable. The ST range between −2 °C and 0 °C can be viewed as an apparent phase transformation temperature interval. Most unfrozen water content froze within this temperature range, and SM decreased rapidly. These results are identical to those of studies on other seasonally freezing regions [33,34]. Moreover, in the winter cooling phase and spring thawing stage, soil heat flow is accompanied by SM migration due to the ST gradient [4]. During the liquid–solid phase changes, soil after long-term straw return exhibited less latent heat consumption (Table 3). A possible reason is that long-term straw return reduced the freezing depth, thereby decreasing the heat consumption during the phase transition. In addition, although we assumed that the moisture–ice phase transition heat in the freezing stage is equivalent to that in the thawing stage, SM variations had different characteristics during the freezing and thawing progress because SM mainly depends on ST [33,35]. Phase-transition heat cannot be estimated because of these characteristics. Phase transition is also associated with vegetation type [23]. Hence, more factors should be considered in analyzing phase-change heat.

4.4. Implication to the Effects of Long-Term Straw Return on the Freeze–Thaw Process

The freeze–thaw process profoundly influences soil hydrothermal conditions and properties in agricultural seasonal freezing–thawing areas [9,36] and can affect soil nutrient and fertility recovery during the fallow period [37]. In recent decades, under the influence of climate warming, the duration of the soil freeze–thaw process has been shortened, and thus the moisture storage effect of the process weakens; this effect causes soil water loss in spring [4]. In addition, the study region is in north–central northeast China, which has low precipitation in the spring. A decrease in infiltrated water may result in insufficient moisture and affect crop seedling growth. Some studies have demonstrated that straw return can inhibit soil evaporation in the thawing stage. For instance, Fu et al. [13] found that straw mulching delays the peak of SM and reduces cumulative evaporation by at least 2.7 mm during the thawing process. During the thawing period, germination and root growth of crops are adversely affected because ST rapidly drops at night and because of late-spring frost [38]. Long-term straw return could reduce temperature fluctuations and freezing intensity. These effects help crop seedlings mitigate soil stress changes during freeze–

thaw cycles. Therefore, straw return has essential theoretical and practical significance for efficiently utilizing soil moisture–heat resources in the seasonal freeze–thaw period.

5. Conclusions

We evaluated the soil heat and moisture dynamics characteristics in the SF and NF during the freeze–thaw process using the observation data on the ST and SM of different profiles based on a 29-year experiment. The results showed that the ST and SM differed between the SF and NF. The soil in both sites had unidirectional freezing and bidirectional melting processes. Long-term straw return delayed soil freezing and thawing, reduced freezing depth, and slowed surface soil freezing rates. It also decreased soil temperature fluctuations and heat exchange efficiency during the freeze–thaw period. Both sites showed decreased SM before the temperature started to freeze at different depths. The migrated SM in most soil layers decreased over the freezing–thawing process in the SF and NF. SM was exponentially related to negative ST at frozen soil depths in both sites. At the −2–0 °C temperature interval, the SM at the 10–30 cm soil layers declined faster than the lower layers in the SF and NF. The energy consumed during the phase change in the SF was lower than that in the NF (33.0 and 43.6 MJ m^{-2}, respectively). Overall, long-term straw return changed the soil freeze–thaw process and hydrothermal characteristics.

Supplementary Materials: The following supporting information can be downloaded at: https://www.mdpi.com/article/10.3390/agronomy14071525/s1, Figure S1: Variations in air temperature and precipitation from 1 May 2019 to 31 May 2020; Table S1: Linear regressions of air temperature and soil temperature; Table S2: Fitting soil moisture with soil temperature in different soil depths.

Author Contributions: Conceptualization, H.L. and M.L.; validation, M.L. and S.W.; formal analysis, H.L. and M.G.; investigation, H.L. and M.G.; resources, M.L.; data curation, H.L.; writing—original draft preparation, H.L.; writing—review and editing, M.L. and S.W.; visualization, H.L.; supervision, M.L. and S.W.; project administration, M.L.; funding acquisition, M.L. All authors have read and agreed to the published version of the manuscript.

Funding: This research was funded by National Key Research and Development Program (Grant NO. 2022YFD1500304; 2021YFD1500702).

Data Availability Statement: The original contributions presented in the study are included in the article and Supplementary Material. Further inquiries can be directed to the corresponding author.

Acknowledgments: The authors are grateful to Xinchun Lu for the support and assistance provided with the data analysis in our manuscript.

Conflicts of Interest: The authors declare no conflicts of interest.

References

1. Meng, F.X.; Hou, R.J.; Li, T.X.; Fu, Q. Variability of soil water heat and energy transfer under different cover conditions in a seasonally frozen soil area. *Sustainability* **2020**, *12*, 1782. [CrossRef]
2. Wang, T.; Li, P.; Li, Z.B.; Hou, J.M.; Xiao, L.; Ren, Z.P.; Xu, G.C.; Yu, K.X.; Su, Y.Y. The effects of freeze-thaw process on soil water migration in dam and slope farmland on the Loess Plateau, China. *Sci. Total Environ.* **2019**, *666*, 721–730. [CrossRef] [PubMed]
3. Sun, L.B.; Chang, X.M.; Yu, X.X.; Jia, G.D.; Chen, L.H.; Wang, Y.S.; Liu, Z.Q. Effect of freeze-thaw processes on soil water transport of farmland in a semi-arid area. *Agric. Water Manag.* **2021**, *252*, 106876. [CrossRef]
4. Yang, K.; Wang, C.H. Water storage effect of soil freeze-thaw process and its impacts on soil hydro-thermal regime variations. *Agric. For. Meteorol.* **2019**, *265*, 280–294. [CrossRef]
5. Maurer, G.E.; Bowling, D.R. Seasonal snowpack characteristics influence soil temperature and water content at multiple scales in interior western U.S. mountain ecosystems. *Water Reour. Res.* **2014**, *50*, 5216–5234. [CrossRef]
6. Fu, Q.; Hou, R.J.; Li, T.J.; Jiang, R.Q.; Yan, P.R.; Ma, Z.A.; Zhou, Z.Q. Effects of soil water and heat relationship under various snow cover during freezing-thawing periods in Songnen Plain, China. *Sci. Rep.* **2018**, *8*, 1325. [CrossRef] [PubMed]
7. Yi, J.; Zhao, Y.; Shao, M.A.; Zhang, J.G.; Cui, L.L.; Si, B.C. Soil freezing and thawing processes affected by the different landscapes in the middle reaches of Heihe River Basin, Gansu, China. *J. Hydrol.* **2014**, *519*, 1328–1338. [CrossRef]
8. Ala, M.; Liu, Y.; Wang, A.Z.; Niu, C.Y. Characteristics of soil freeze–thaw cycles and their effects on water enrichment in the rhizosphere. *Geoderma* **2016**, *264*, 132–139. [CrossRef]

9. Chen, S.Y.; Ouyang, W.; Hao, F.H.; Zhao, X.C. Combined impacts of freeze–thaw processes on paddy land and dry land in Northeast China. *Sci. Total Environ.* **2013**, *456–457*, 24–33. [CrossRef]
10. Chen, J.F.; Wang, E.Q.; Xue, J.; Cui, L.H.; Zheng, X.Q.; Du, Q. Effects of soil particle size and gradation on the transformation between shallow phreatic water and soil water under laboratory freezing-thawing action. *J. Hydrol.* **2023**, *619*, 129323. [CrossRef]
11. Wang, W.N.; Wang, W.S.; Wang, P.; Wang, X.H.; Wang, L.W.; Wang, C.Z.; Zhang, C.L.; Huo, Z.L. Impact of straw return on soil temperature and water during the freeze-thaw period. *Agric. Water Manag.* **2023**, *282*, 108292. [CrossRef]
12. Bristow, K. The role of mulch and its architecture in modifying soil temperature. *Soil Res.* **1988**, *26*, 269–280. [CrossRef]
13. Fu, Q.; Yan, P.R.; Li, T.X.; Cui, S.; Peng, L. Effects of straw mulching on soil evaporation during the soil thawing period in a cold region in northeastern China. *J. Earth Syst. Sci.* **2018**, *127*, 33. [CrossRef]
14. Song, X.L.; Sun, R.J.; Chen, W.F.; Wang, M.H. Effects of surface straw mulching and buried straw layer on soil water content and salinity dynamics in saline soils. *Can. J. Soil Sci.* **2019**, *100*, 58–68. [CrossRef]
15. Cui, S.Y.; Cao, G.Q.; Zhu, X.K. Evaluation of ecosystem service of straw return to soil in a wheat field of China. *Int. J. Agric. Biol. Eng.* **2021**, *14*, 192–198. [CrossRef]
16. Liu, S.C.; Zhang, H.; Lyu, J.L.; Wang, Y.Y.; Guo, W.L. A preliminary study on soil water transport and thermodynamics in a Loess soil with straw returning for long time. *J. Agro-Environ. Sci.* **2012**, *31*, 1791–1798. (In Chinese) [CrossRef]
17. Ma, Y.Z.; Zhang, Y.S.; Zubrzycki, S.; Guo, Y.H.; Farhan, S.B. Hillslope-scale variability in seasonal frost depth and soil water content investigated by GPR on the southern margin of the sporadic permafrost zone on the Tibetan Plateau. *Permafrost Periglac. Process.* **2015**, *26*, 321–334. [CrossRef]
18. Liu, X.B.; Burras, C.L.; Kravchenko, Y.S.; Duran, A.; Huffman, T.; Morras, H.; Studdert, G.; Zhang, X.Y.; Cruse, R.M.; Yuan, X.H. Overview of Mollisols in the world: Distribution, land use and management. *Can. J. Soil Sci.* **2012**, *92*, 383–402. [CrossRef]
19. Li, T.X.; Yu, P.F.; Liu, D.; Fu, Q.; Hou, R.J.; Zhao, H.; Xu, S.; Zuo, Y.T.; Xue, P. Effects of biochar on sediment transport and rill erosion after two consecutive years of seasonal freezing and thawing. *Sustainability* **2021**, *13*, 6984. [CrossRef]
20. Tian, P.; Lian, H.L.; Wang, Z.Y.; Jiang, Y.; Li, C.F.; Sui, P.X.; Qi, H. Effects of deep and shallow tillage with straw incorporation on soil organic carbon, total nitrogen and enzyme activities in Northeast China. *Sustainability* **2020**, *12*, 8679. [CrossRef]
21. Zhang, J.; Hang, X.N.; Lamine, S.M.; Jiang, Y.; Afreh, D.; Qian, H.Y.; Feng, X.M.; Zheng, C.Y.; Deng, A.X.; Song, Z.W.; et al. Interactive effects of straw incorporation and tillage on crop yield and greenhouse gas emissions in double rice cropping system. *Agric. Ecosyst. Environ.* **2017**, *250*, 37–43. [CrossRef]
22. Anderson, D.M.; Tice, A.R. Physical aspects of soil water and salts in ecosystems. In *The Unfrozen Interfacial Phase in Frozen Soil Water Systems*; Springer: Berlin/Heidelberg, Germany, 1973; pp. 107–124.
23. Hu, G.J.; Zhao, L.; Wu, X.D.; Li, R.; Wu, T.H.; Xie, C.W.; Pang, Q.Q.; Xiao, Y.; Li, W.P.; Qiao, Y.P.; et al. Modeling permafrost properties in the Qinghai-Xizang (Tibet) Plateau. *Sci. China Earth Sci.* **2015**, *58*, 2309–2326. [CrossRef]
24. Tian, H.H.; Wei, C.F.; Wei, H.Z.; Zhou, J.Z. Freezing and thawing characteristics of frozen soils: Bound water content and hysteresis phenomenon. *Cold Reg. Sci. Technol.* **2014**, *103*, 74–81. [CrossRef]
25. Wang, G.P.; Ke, Q.H.; Zhang, K.L.; Li, Y.T.; Liu, H.Y.; Yu, Y.; Ma, Q.H. Responses of freeze-thaw process and hydrothermal variations within soil profiles to the cultivation of forest and grassland in Northeast China. *Soil Tillage Res.* **2023**, *228*, 105653. [CrossRef]
26. Zhao, L.; Hu, G.J.; Wu, X.D.; Wu, T.H.; Li, R.; Pang, Q.Q.; Zou, D.E.; Du, E.J.; Zhu, X.F. Dynamics and characteristics of soil temperature and moisture of active layer in the central Tibetan Plateau. *Geoderma* **2021**, *400*, 115083. [CrossRef]
27. Mu, Y.T.; Liu, Z.Q.; Li, Y.; Zhu, D.Y. Characteristics of soil temperature variation in karst area and its relationship with environmental factors. *Acta Ecol. Sin.* **2021**, *41*, 2738–2749. (In Chinese) [CrossRef]
28. Liu, S.; Huang, Q.Z.; Ren, D.Y.; Xu, X.; Xiong, Y.W.; Huang, G.H. Soil evaporation and its impact on salt accumulation in different landscapes under freeze–thaw conditions in an arid seasonal frozen region. *Vadose Zone J.* **2021**, *20*, e20098. [CrossRef]
29. Li, X.; Jin, R.; Pan, X.D.; Zhang, T.J.; Guo, J.W. Changes in the near-surface soil freeze-thaw cycle on the Qinghai-Tibetan Plateau. *Int. J. Appl. Earth Obs. Geoinf.* **2012**, *17*, 33–42. [CrossRef]
30. Fu, Q.; Wang, X.H.; Liu, D.; Li, T.X. Thermal condition of snow and its response to meteorological factors at field scale. *Trans. ASABE* **2016**, *59*, 903–912. [CrossRef]
31. Nagare, R.M.; Schincariol, R.A.; Quinton, W.L.; Hayashi, M. Effects of freezing on soil temperature, freezing front propagation and moisture redistribution in peat: Laboratory investigations. *Hydrol. Earth Syst. Sci.* **2012**, *16*, 501–515. [CrossRef]
32. Hinkel, K.M.; Outcalt, S.I.; Nelson, F.E. Temperature variation and apparent thermal diffusivity in the refreezing active layer, Toolik Lake, Alaska. *Permafrost Periglac. Process.* **1990**, *1*, 265–274. [CrossRef]
33. Hu, G.J.; Zhao, L.; Zhu, X.F.; Wu, X.D.; Wu, T.H.; Li, R.; Xie, C.W.; Hao, J.M. Review of algorithms and parameterizations to determine unfrozen water content in frozen soil. *Geoderma* **2020**, *368*, 114277. [CrossRef]
34. Zhang, Y.S.; Wang, S.S.; Barr, A.G.; Black, T.A. Impact of snow cover on soil temperature and its simulation in a boreal aspen forest. *Cold Reg. Sci. Technol.* **2008**, *52*, 355–370. [CrossRef]
35. Yuan, L.M.; Zhao, L.; Li, R.; Hu, G.J.; Du, E.J.; Qiao, Y.P.; Ma, L. Spatiotemporal characteristics of hydrothermal processes of the active layer on the central and northern Qinghai–Tibet plateau. *Sci. Total Environ.* **2020**, *712*, 136392. [CrossRef]
36. He, Z.; Hou, R.J.; Fu, Q.; Li, T.X.; Zhang, S.J.; Su, A.S. Evolution mechanism of soil hydrothermal parameters under freeze–thaw cycles: Regulatory significance of straw and biochar. *J. Clean. Prod.* **2023**, *385*, 135787. [CrossRef]

37. Fu, Q.; Li, T.N.; Li, T.X.; Cui, H. Influence of straw mulching on soil moisture characteristics during seasonal freeze-thaw period. *Trans. Chin. Soc. Agric. Mach.* **2015**, *46*, 141–146. (In Chinese) [CrossRef]
38. Yin, W.; Chai, Q.; Guo, Y.; Fan, Z.L.; Hu, F.L.; Fan, H.; Zhao, C.; Yu, A.Z.; Coulter, J.A. Straw and plastic management regulate air-soil temperature amplitude and wetting-drying alternation in soil to promote intercrop productivity in arid regions. *Field Crops Res.* **2020**, *249*, 107758. [CrossRef]